EPR Studies of Oxo−Molybdenum(V) Complexes with Sulfur Donor Ligands: Implications for the Molybdenum Center of Sulfite Oxidase

Ish K. Dhawan and John H. Enemark*

Department of Chemistry, University of Arizona, Tucson, Arizona 85721

Received May 10, 1996[⊗]

A series of six-coordinate compounds containing a chelating dithiolate coordinated to the $[LMo^{V}O]^{2+}$ unit (L = hydrotris(3,5-dimethyl-1-pyrazolyl)borate) have been characterized by EPR spectroscopy as models for the molybdenum centers of pterin-containing molybdenum enzymes. The structure of LMoO(bdt) (**1**) (bdt = 1,2-benzenedithiolate) has been determined by X-ray crystallography; the space group is $P2_1/n$ with $a = 10.727(1)$ Å, $b = 14.673(2)$ Å, $c = 15.887(2)$ Å, $\beta = 100.317(4)°$ and $Z = 4$. Compound **1** exhibits distorted octahedral stereochemistry; the terminal oxo group and the sulfur atoms are mutually cis to one another. The Mo═O distance is 1.678(4) Å, and the average Mo−S distance is 2.373(2) Å. The EPR parameters for **1**, determined from simulation of the frozen-solution spectrum, are $g_1 = 2.004$, $g_2 = 1.972$, $g_3 = 1.934$ and $A_1(^{95,97}\text{Mo}) = 50.0 \times 10^{-4}$, $A_2 = 11.4 \times 10^{-4}$, $A_3 = 49.7 \times 10^{-4}$ cm^{-1}. The EPR parameters for several $LMo^{V}O\{S(CH_2)_xS\}$ compounds ($x = 2-4$) with saturated chelate skeletons are similar to those of **1**, indicating that it is the coordinated S atoms and not unsaturation of the chelate skeleton that gives rise to the large g values for **1**. The presence of g components larger than the free-electron value is ascribed to low-energy charge transfer transitions from the filled sulfur π orbitals to half-filled Mo d orbitals. The EPR spectrum of $[LMo^{V}O\{S_2P(OEt)_2\}]^{+}$ shows an unusually large isotropic ^{31}P hyperfine splitting of 66.1×10^{-4} cm^{-1} from the noncoordinated phosphorus atom. The frozen-solution EPR spectra of the low-pH and high-pH forms of sulfite oxidase have been reinvestigated in D_2O and the anisotropic g and $A(^{95,97}\text{Mo})$ parameters determined by simulation of the spectrum arising from the naturally abundant Mo isotopes (75% $I = 0$, 25% $I = {}^5/_2$). The EPR parameters for the low-pH form are $g_1 = 2.007$, $g_2 = 1.974$, $g_3 = 1.968$ and $A_1 = 56.7 \times 10^{-4}$, $A_2 = 25.0 \times 10^{-4}$, $A_3 = 16.7 \times 10^{-4}$ cm^{-1}. The EPR parameters for the high-pH form are $g_1 = 1.990$, $g_2 = 1.966$, $g_3 = 1.954$ and $A_1 = 54.4 \times 10^{-4}$, $A_2 = 21.0 \times 10^{-4}$, $A_3 = 11.3 \times 10^{-4}$ cm^{-1}. These are the first determinations of the complete $A(^{95,97}\text{Mo})$ hyperfine components for an enzyme that possesses an $[Mo^{VI}O_2]^{2+}$ core in its fully oxidized state.

Introduction

Pterin-containing molybdoenzymes (e.g. sulfite oxidase, xanthine oxidase, nitrate reductase) catalyze a variety of two-electron reactions involving net transfer of an oxygen atom between substrate and water.[1−5] These enzymes are proposed to possess a common molybdenum cofactor (Mo-co) in which the molybdenum atom is coordinated by the two sulfur atoms from the *cis*-enedithiolate function of the novel 6-substituted pterin (molybdopterin),[6] as shown in Figure 1a. The *cis*-dithiolate coordination of molybdopterin was first confirmed by the X-ray crystal structure of the tungsten-containing enzyme aldehyde ferredoxin oxidoreductase (AOR) from *Pyrococcus furiosus*, which contains *two* molybdopterin ligands per tungsten atom.[7] More recently, crystallographic results became available for two molybdenum-containing enzymes. Aldehyde oxidoreductase from *Desulfovibrio gigas* possesses a *single* molybdopterin cytosine dinucleotide per molybdenum atom,[8] whereas dimethyl sulfoxide (DMSO) reductase from *Rhodobacter sphaeroides* has *two* molybdopterin guanine dinucleotide units per molybdenum atom.[9] In all of these enzyme structures, the molybdopterin unit adopts a tricyclic structure with a pyran

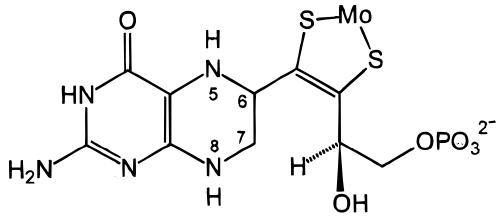

a

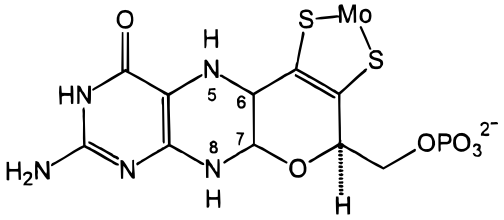

b

Figure 1. (a) Molybdopterin complex originally proposed from degradative studies,[6] showing the enedithiolate coordination of a molybdenum atom. (b) Molybdopterin coordination found in enzymes,[7−9] showing the tricylic structure involving a pyran linkage at C7. In some enzymes the phosphate group is replaced by a dinucleotide. Aldehyde oxidoreductase from *D. gigas* has one molybdopterin cytosine dinucleotide per molybdenum;[8] DMSO reductase has two molybdopterin guanine dinucleotides coordinated to one molybdenum atom.[9]

[⊗] Abstract published in *Advance ACS Abstracts,* August 1, 1996.

(1) Spiro, T. In *Molybdenum Enzymes*; John Wiley and Sons: New York, 1985.
(2) Enemark, J. H.; Young, C. G. *Adv. Inorg. Chem.* **1993**, *40*, 1−88.
(3) Pilato, R. S.; Stiefel, E. I. In *Bioinorganic Catalysis*; Reedijk, J., Ed.; Marcel Dekker, Inc.: New York, 1993; pp 131−188.
(4) Holm, R. H. *Coord. Chem. Rev.* **1990**, *100*, 183.
(5) *Molybdenum and Molybdenum-containing Enzymes*; Coughlan, M., Ed.; Pergamon Press: New York, 1980.
(6) Rajagopalan, K. V. *Adv. Enzymol. Relat. Areas Mol. Biol.* **1991**, *64*, 215−290.
(7) Chan, M. K.; Mukund, S.; Kletzin, A.; Adams, M. W. W.; Rees, D. C. *Science* **1995**, *267*, 1463.
(8) Romão, M. J.; Archer, M.; Moura, I.; Moura, J. J. G.; LeGall, J.; Engh, R.; Schneider, M.; Hof, P.; Huber, R. *Science* **1995**, *270*, 1170−1176.

S0020-1669(96)00527-7 CCC: $12.00

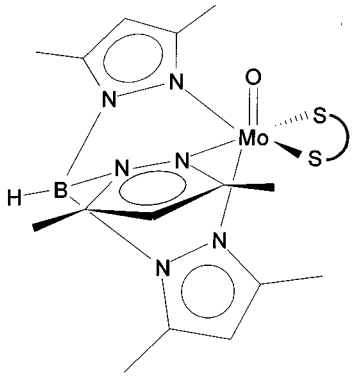

Figure 2. Stereochemistry of the $[LMo^{V}O]^{2+}$ complexes (L = hydrotris(3,5-dimethyl-1−pyrazolyl)borate). S⁀S represents the various bidentate sulfur donor ligands.

linkage at C7 (Figure 1b) rather than the open-chain structure (Figure 1a) originally deduced from degradative studies by Rajagopalan and co-workers.[6]

The presence of two coordinated sulfur atoms in aldehyde oxidoreductase from *D. gigas*[8] compared to four coordinated sulfur atoms in DMSO reductase from *R. sphaeroides*[9] renews interest in determining the total number of sulfur atoms coordinated to the molybdenum atom at the active sites of other pterin-containing molybdoenzymes. For sulfite oxidase, EXAFS studies[10,11] at the Mo K-edge and EPR studies[12,13] of the transient molybdenum(V) states that appear during enzyme turnover support an oxo−molybdenum active site with at least two sulfur donor atoms and a coordinated OH group. The EPR parameters of molybdenum centers are sensitive to the number of coordinated sulfur atoms, and extensive model studies have been done to mimic the molybdenum(V) states of enzymes.[2,14,15] Unfortunately, in most of the model studies complete EPR parameters, including the anisotropic $A(^{95,97}Mo)$ hyperfine splittings, have not been determined by spectral simulation. One exception is the series of elegant studies by Wedd and co-workers[16−18] on isotopically labeled model oxo−molybdenum(V) complexes that mimic the EPR parameters of xanthine oxidase.

Here we report the first structurally characterized monooxo−molybdenum(V) complex that possesses a *single dithiolene* ligand, the *minimum structural feature* for the Mo(V) state of a pterin-containing molybdenum enzyme. In addition, we have carried out detailed EPR studies of other members of a series of well-characterized neutral and cationic six-coordinated oxo−molybdenum(V) complexes that possess a single bidentate sulfur donor ligand and which exhibit a range of chelate ring sizes possessing saturated and unsaturated ligand skeletons (Figure 2). We have also reinvestigated and simulated the EPR parameters of $[MoO(edt)_2]^-$, in which four sulfur atoms are coordinated to the molybdenum center, as found in the X-ray structure of DMSO reductase[9] and the tungsten-containing aldehyde ferredoxin oxidoreductase.[7]

The EPR spectra of the high- and low-pH forms of sulfite oxidase have been reinvestigated in D_2O in order to eliminate the strong hyperfine splitting from the exchangeable proton of the coordinated OH group.[11−14] These experiments have enabled all three $A(^{95,97}Mo)$ hyperfine splittings for these forms of sulfite oxidase to be determined for the first time by spectral simulation of the *natural-mixed-isotope* spectra. These EPR parameters for the molybdenum center of sulfite oxidase, whose structure is unknown, are compared to the parameters of well-characterized model complexes with two, three, and four sulfur donor atoms and to the available EPR parameters of aldehyde oxidoreductase from *D. gigas*,[19] which was recently shown by X-ray crystallography to have two sulfur atoms coordinated to the molybdenum atom.[8] A preliminary account of portions of this work has appeared.[20]

Experimental Section

Solvents were purified by distillation as follows: acetonitrile from calcium hydride; chloroform from anhydrous calcium chloride; toluene from sodium. Anhydrous *N*,*N*-dimethylformamide was obtained from Aldrich Chemical Co. and used as received. Deuterium oxide (99.9%) was from Cambridge Isotope Laboratories; buffers and reagents were obtained from Sigma and used as received.

Abbreviations. L = hydrotris(3,5-dimethyl-1-pyrazolyl) borate; bdt = 1,2-benzenedithiolate; edt = ethanedithiolate.

Syntheses. The syntheses of LMoO(bdt) (**1**), LMoO(edt) (**2**), $LMoO\{S(CH_2)_3S\}$ (**3**), and $LMoO\{S(CH_2)_4S\}$ (**4**) followed previous methods.[21,22] The cationic Mo(V) complexes $[LMo^{V}O(S_2CNEt_2)]^+$ (**5**) and $[LMo^{V}O\{S_2P(OEt)_2\}]^+$ (**6**) were generated in solution by one-electron electrochemical oxidation of $LMo^{IV}O(S_2CNEt_2)$[23] and $LMo^{IV}O\{S_2P(OEt)_2\}$,[24] respectively, and $[PPh_4][MoO(edt)_2]$ (**7**) was synthesized by literature methods.[25]

Sulfite Oxidase. Chicken liver sulfite oxidase (SO) was purified by the method of Sullivan *et al.*;[26] the enzyme used for the EPR experiment showed a heme to protein absorbance ratio (A_{414}/A_{280}) of 0.81.

EPR Measurements. Samples of **1**−**4** were prepared as 1 mM solutions in toluene. Cationic complexes (**5** and **6**) were generated electrochemically in acetonitrile solution and immediately subjected to EPR measurements. For **7**, a 3/1 acetonitrile/DMF mixture was used.

The low-pH form of SO was generated by the following method. A 0.1 M Tris−DCl buffer, pD = 7.0, containing 1 mM EDTA, was prepared by adjusting the pD of a 0.1 M Tris−DCl solution with a 0.1 M solution of Tris base in D_2O. The pD value was arrived at by adding 0.4 pH unit to the pH reading obtained with a glass electrode (Sigma, E 4878, calomel).[27,28] A sample of SO was prepared for EPR analysis by repeatedly diluting 10 μL of stock SO with 1 mL of the Tris−DCl buffer and then reconcentrating the sample using a Centricon 30 (Amicon) ultrafiltration device to approximately 0.1 mM in SO. The SO was reduced immediately before the EPR experiment by adding 10 μL of 0.106 M Na_2SO_3 in D_2O to 100 μL of SO solution. The reduced SO was frozen in liquid nitrogen 2 min after addition of sulfite.

(9) Schindelin, H.; Kisker, C.; Hilton, J.; Rajagopalan, K. V.; Rees, D. C. *Science* **1996**, *272*, 1615−1621.
(10) Cramer, S. P.; Wahl, R.; Rajagopalan, K. V. *J. Am. Chem. Soc.* **1981**, *103*, 7721−7727.
(11) George, G. N.; Kipke, C. A.; Prince, R. C.; Sunde, R. A.; Enemark, J. H.; Cramer, S. P. *Biochemistry* **1989**, *28*, 5075.
(12) Bray, R. C. *Biol. Magn. Reson.* **1980**, *2*, 45.
(13) George, G. N.; Bray, R. C. *Biochemistry* **1988**, *27*, 3603.
(14) Bray, R. C. *Q. Rev. Biophys.* **1988**, 299−329.
(15) Carducci, M. D.; Enemark, J. H. Manuscript in preparation.
(16) Wilson, G. J.; Greenwood, R. J.; Pilbrow, J. R.; Spence, J. T.; Wedd, A. G. *J. Am. Chem. Soc.* **1991**, *113*, 6803−6812.
(17) Greenwood, R. J.; Wilson, G. L.; Pilbrow, J. R.; Wedd, A. G. *J. Am. Chem. Soc.* **1993**, *115*, 5385−5392.
(18) Wilson, G. L.; Kony, M.; Tiekink, E. R. T.; Pilbrow, J. R.; Spence, J. T.; Wedd, A. G. *J. Am. Chem. Soc.* **1988**, *110*, 6923.
(19) Turner, N.; Barata, B.; Bray, R. C.; Deistung, J.; LeGall, J. *Biochem. J.* **1987**, *243*, 755−761.
(20) Dhawan, I. K.; Pacheco, A.; Enemark, J. H. *J. Am. Chem. Soc.* **1994**, *116*, 7911−7912.
(21) Cleland, W. E., Jr.; Barnhart, K. M.; Yamanouchi, K.; Collison, D.; Mabbs, F. E.; Ortega, R. B.; Enemark, J. H. *Inorg. Chem.* **1987**, *26*, 1017−1025.
(22) Chang, C. S. J.; Collison, D.; Mabbs, F. E.; Enemark, J. H. *Inorg. Chem.* **1990**, *29*, 2261−2267.
(23) Young, C. G.; Roberts, S. A.; Ortega, R. B.; Enemark, J. H. *J. Am. Chem. Soc.* **1987**, *109*, 2938−2946.
(24) Roberts, S. A.; Young, C. G.; Cleland, W. E., Jr.; Ortega, R. B.; Enemark, J. H. *Inorg. Chem.* **1988**, *27*, 3044.
(25) Ellis, S. R.; Collison, D.; Garner, C. D.; Clegg, W. *J. Chem. Soc., Chem. Commun.* **1986**, 1483−1485.
(26) Sullivan, E. P., Jr.; Hazzard, J. T.; Tollin, G.; Enemark, J. H. *Biochemistry* **1993**, *32*, 12465−12470.
(27) Cohen, H. J.; Fridovich, I.; Rajagopalan, K. V. *J. Biol. Chem.* **1971**, *246*, 374.
(28) Glascoe, P. K.; Long, F. A. *J. Phys. Chem.* **1960**, *64*, 188.

A similar method was followed to prepare the sample for the high-pH form of SO, except that Bis-Tris propane was used to prepare the solutions at pH 9.5. The pH of the buffer was adjusted using 6 M HCl.

EPR spectra were obtained at room temperature and at 77 K on a Bruker ESP 300E spectrometer operating at X-band (ca. 9.1 GHz). Frequencies were measured with a Systron Donner-6530 frequency counter.

Analysis of EPR Spectra. The frozen-solution EPR spectra were simulated with a modified version of the program QPOW developed by Prof. R. L. Belford and co-workers.[29,30] Computations were performed on CONVEX C210 and IBM RISC 6000-590 computers in the Center for Computing and Information Technology (CCIT) and the Department of Chemistry at the University of Arizona. The spectral simulations were achieved by using the spin Hamiltonian of eq 1, where

$$H = \beta H(g_{xx}\hat{S}_x + g_{yy}\hat{S}_y + g_{zz}\hat{S}_z) + A_{XX}\hat{S}_X\hat{I}_X + A_{YY}\hat{S}_Y\hat{I}_Y + A_{ZZ}\hat{S}_Z\hat{I}_Z \quad (1)$$

all symbols have their usual meanings. Anisotropic g values and the approximate line widths ($I = 0$ component) were first directly obtained from the frozen-solution EPR spectra and then simulated ($I = 0$ component only) to obtain the best visual fit. Both the anisotropic g values and line widths were varied until satisfactory fits of the spectra were obtained. Preliminary $A(^{95,97}\text{Mo})$ values were obtained from the frozen-solution spectra when possible. In most cases, only two of the principal A values could be measured, so the third was approximated by the relation $\langle A\rangle = (A_{XX} + A_{YY} + A_{ZZ})/3$ where $\langle A\rangle$ is the isotropic ^{95,97}Mo hyperfine value observed at room temperature. Where possible, the approximate line widths of the $A(^{95,97}\text{Mo})$ hyperfine splittings were measured from the experimental spectrum. The anisotropic $A(^{95,97}\text{Mo})$ components were then simulated separately ($I = {}^5/_2$ component only) until the best fit was observed for these features of the spectrum. The anisotropic g values were kept fixed at the values previously determined for the $I = 0$ component. In the simulation of the $I = {}^5/_2$ contributions, the three anisotropic $A(^{95,97}\text{Mo})$ components and the line widths were first varied to obtain a reasonable fit. Low-symmetry oxo−molybdenum(V) complexes may have noncoincident **g** and $\mathbf{A}(^{95,97}\text{Mo})$ tensors; the three Euler angles (α, β, and γ) transform the $\mathbf{A}(^{95,97}\text{Mo})$ tensor into the **g**-tensor axis system (in the case of C_s symmetry only β is needed). In addition to $A(^{95,97}\text{Mo})$ values and line widths, Euler angles were varied until the best fit was observed. About 60−70 simulation trials were required to achieve a satisfactory fit for each spectrum. Finally, each simulated spectrum ($I = 0$ and $I = {}^5/_2$ components) was integrated separately and the contributions from the $I = {}^5/_2$ (^{95,97}Mo isotopes, 25% abundant) and $I = 0$ (^{92,94,96,98}Mo isotopes, 75% abundant) components were summed, taking into account their natural abundances. The derivative of the composite simulated spectrum was obtained and compared to the experimental spectrum.

Structure Determination. Crystal data and details of the structure determinations are given in Table 1. Scattering factors were taken from Cromer and Waber,[31] anomalous dispersion effects were included for all non-hydrogen atoms with the values of $\Delta f'$ and $\Delta f''$ taken from Cromer,[32] and all calculations were performed on a VAX using MolEN (Enraf-Nonius).

Results and Discussion

Structure of LMoO(bdt). The structure of LMoO(bdt), determined by single-crystal X-ray diffraction, is shown in Figure 3. Positional parameters and selected bond distances and angles are shown in Tables 2 and 3, respectively. The terminal oxo group and the two sulfur atoms are constrained to be mutually cis to one another by the *fac* stereochemistry imposed by L. The Mo═O and Mo−N distances agree with those for related Mo(V) complexes.[21,33] The two Mo−S distances (Table 3) (2.373(2) Å average) are slightly shorter than the average Mo−S distance (2.382(2) Å) in a six-coordinate oxo−molybdenum(V) complex with similar cis coordination of the sulfur atoms.[21] Six-coordinate oxo−molybdenum(V) complexes in which the two sulfur atoms are trans to one another have Mo−S distances in the range 2.403−2.462 Å.[18,34] In the five-coordinate oxo−molybdenum(V) complexes, $[MoO(edt)_2]^-$ [25] and $[MoO(bdt)_2]^-$,[35] the average Mo−S distances are 2.372(3) and 2.377(3) Å, respectively, and in $[MoO(SPh)_4]^-$, the average Mo−S distance is 2.403(5) Å.[36] In general, Mo−S distances in nonchelated thiolates are slightly longer than those for chelated 1,2-dithiolates or 1,2-arenedithiolates. The Mo−S distances obtained from the EXAFS studies of the Mo(V) state of sulfite oxidase are in the range 2.38−2.41 Å.[11]

The effective coordination symmetry of the molybdenum center is C_s. The bond angles about the molybdenum atom deviate significantly from octahedral geometry. The large S−Mo−O angles (S1−Mo−O = 101.2(2)° and S2−Mo−O =

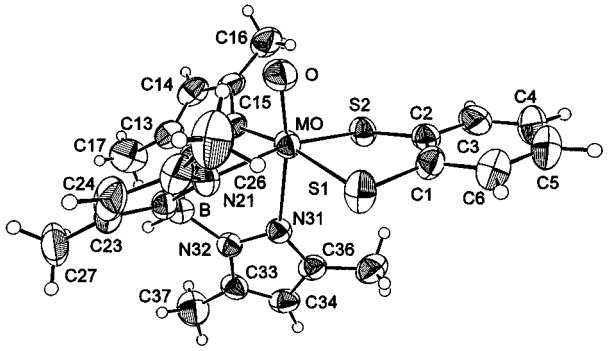

Figure 3. ORTEP drawing of LMoO(bdt) (**1**). The atoms are drawn as 50% probability ellipsoids, and H atom radii have been reduced for clarity.

Table 1. Summary of Crystal Data for LMoO(bdt), **1**

empirical formula	$MoS_2ON_6C_{21}BH_{26}$
fw	549.36
$F(000)$	1124
crystal dimens	0.10 × 0.12 × 0.30 mm
peak width at half-height	0.27°
λ(Mo Kα)	0.71073 Å
temperature	23 ± 1 °C
crystal class	monoclinic
space group	$P2_1/n$
cell params	$a = 10.727(1)$ Å
	$b = 14.673(2)$ Å
	$c = 15.887(2)$ Å
	$\beta = 100.317(4)°$
	$V = 2460(3)$ Å^3
	$Z = 4$
calcd density	1.479 g/cm^3
obsd density	1.482 g/cm^3
abs. coff., μ	6.596 cm^{-1}
no. of reflns. measd, unique	4789, 4339
no. of reflns. included	2708 with $F_o^2 > 2.0\sigma(F_o^2)$
no. of params refined	289
unweighted agreement factor	0.041
weighted agreement factor	0.051
esd in observn of unit weight	1.27

(29) Computer Simulation of Powder Spectra. Belford, R. L.; Nilges, M. J. EPR Symposium, 21st Rocky Mountain Conference, Denver, CO, 1979.
(30) Nilges, M. J. Ph.D. Dissertation, University of Illinois, Urbana, IL, 1979.
(31) Cromer, D. T.; Waber, J. T. *International Tables for X-ray Crystallography*; Kynoch: Birmingham, England, 1974; Vol. IV, Table 2.2B.
(32) Cromer, D. T. *International Tables for X-ray Crystallography*; Kynoch: Birmingham, England, 1974; Vol. IV, Table 2.3.1.
(33) Basu, P.; Bruck, M. A.; Li, Z.; Dhawan, I. K. *Inorg. Chem.* **1995**, *34*, 405−407.
(34) Yamanouchi, K.; Enemark, J. H. *Inorg. Chem.* **1979**, *18*, 1626−1633.
(35) Boyde, S.; Ellis, S. R.; Garner, C. D.; Clegg, W. *J. Chem. Soc., Chem. Commun.* **1986**, 1541−1543.
(36) Bradbury, J. R.; Mackay, M. F.; Wedd, A. G. *Aust. J. Chem.* **1978**, *31*, 2423.

Table 2. Positional Parameters and Their Estimated Standard Deviations for LMoO(bdt), **1**

atom	*x*	*y*	*z*	B^a (Å^2)
Mo	0.03425(4)	0.21906(3)	−0.12742(3)	3.182(8)
S1	0.2330(1)	0.2298(1)	−0.1718(1)	4.66(4)
S2	0.0193(1)	0.37845(9)	−0.15479(9)	3.88(3)
O	0.0787(4)	0.2188(3)	−0.0206(2)	4.75(9)
N11	−0.1651(4)	0.2091(3)	−0.1169(3)	3.64(9)
N12	−0.2430(4)	0.1430(3)	−0.1603(3)	3.5(1)
N21	0.0289(4)	0.0709(3)	−0.1353(3)	3.33(9)
N22	−0.0782(4)	0.0260(3)	−0.1752(3)	3.10(9)
N31	−0.0578(4)	0.1996(3)	−0.2736(3)	3.16(9)
N32	−0.1536(4)	0.1362(3)	−0.2938(2)	3.10(9)
C1	0.2696(5)	0.3466(4)	−0.1625(3)	3.9(1)
C2	0.1770(5)	0.4115(3)	−0.1556(3)	3.5(1)
C3	0.2094(6)	0.5032(4)	−0.1512(4)	5.2(1)
C4	0.3313(6)	0.5294(4)	−0.1532(4)	6.5(2)
C5	0.4236(6)	0.4664(5)	−0.1574(4)	6.7(2)
C6	0.3925(6)	0.3758(4)	−0.1638(4)	5.3(2)
C13	−0.3566(5)	0.1453(4)	−0.1353(4)	4.3(1)
C14	−0.3515(6)	0.2139(4)	−0.0759(4)	4.9(1)
C15	−0.2341(6)	0.2517(4)	−0.0648(3)	4.3(1)
C16	−0.1817(6)	0.3246(4)	−0.0052(4)	6.0(2)
C17	−0.4620(5)	0.0836(5)	−0.1692(5)	7.1(2)
C23	−0.0651(5)	−0.0639(3)	−0.1587(3)	3.7(1)
C24	0.0517(5)	−0.0759(4)	−0.1090(4)	4.7(1)
C25	0.1082(5)	0.0081(4)	−0.0949(4)	4.1(1)
C26	0.2333(5)	0.0302(4)	−0.0423(4)	5.9(2)
C27	−0.1628(6)	−0.1331(4)	−0.1932(4)	5.7(2)
C33	−0.1984(5)	0.1374(4)	−0.3782(3)	3.8(1)
C34	−0.1328(5)	0.2019(4)	−0.4134(3)	4.1(1)
C35	−0.0457(5)	0.2390(4)	−0.3484(3)	3.6(1)
C36	0.0475(6)	0.3116(4)	−0.3572(4)	5.2(2)
C37	−0.3032(6)	0.0789(4)	−0.4199(4)	6.4(2)
B	−0.1926(6)	0.0790(4)	−0.2230(4)	3.4(1)

[a] Anisotropically refined atoms are given in the form of the isotropic equivalent displacement parameter defined as $(4/3)[a^2B(1,1) + b^2B(2,2) + c^2B(3,3) + ab(\cos\gamma)B(1,2) + ac(\cos\beta)B(1,3) + bc(\cos\alpha)B(2,3)]$.

Table 3. Selected Bond Distances (Å) and Angles (deg) for LMoO(bdt), **1**

Mo−S1	2.368(2)	Mo−S2	2.379(2)
Mo−O	1.678(4)	Mo−N11	2.179(5)
Mo−N21	2.178(4)	Mo−N31	2.372(4)
S1−C1	1.758(6)	S2−C2	1.762(6)
N11−N12	1.382(6)	N12−B	1.536(7)
N21−N22	1.377(6)	N22−B	1.535(7)
N31−N32	1.380(6)	N32−B	1.520(7)
S1−Mo−S2	85.12(6)	S1−Mo−O	101.2(2)
S1−Mo−N11	167.3(1)	S1−Mo−N21	93.7(1)
S1−Mo−N31	87.5(1)	Mo−N31−N32	118.1(3)
S2−Mo−O	100.7(1)	S2−Mo−N11	92.6(1)
S2−Mo−N21	166.1(1)	S2−Mo−N31	86.4(1)
O−Mo−N11	91.6(2)	O−Mo−N21	93.1(2)
O−Mo−N31	169.2(2)	N11−Mo−N21	85.5(2)
N11−Mo−N31	79.9(2)	N21−Mo−N31	79.7(2)
Mo−S1−C1	103.9(2)	Mo−S2−C2	103.8(2)
Mo−N21−N22	121.0(3)	N12−B−N22	109.4(4)
N12−B−N32	108.6(5)	N22−B−N32	110.2(5)
Mo−N11−N12	121.5(3)		

100.7(1)°) can be explained by nonbonded repulsions between the filled pπ orbitals on sulfur and the π-electron density in the Mo═O bond.[34] The molybdenum atom is not in the plane of the benzenedithiolate ligand. The angle between the plane Mo, S1, S2 and the plane containing S1, S2, C1, C2 is 21.3(1)°. This deformation is probably due to nonbonded interaction between the C36 methyl group and atoms C1 and C2 of the benzenedithiolate group. The contact distances between C36···C2 and C36···C1 are 3.57 and 3.58 Å, respectively, less than the estimated van der Waals contact between a methyl group and an aromatic ring (3.7 Å).[37] A similar phenomenon was observed for LMoO(catCl_4).[33]

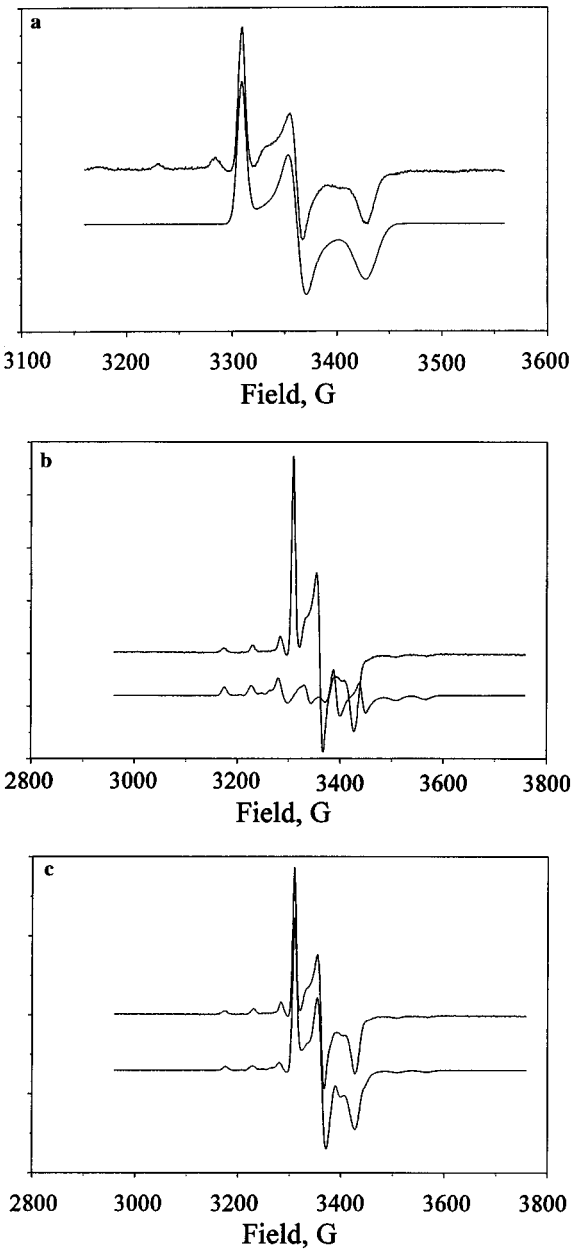

Figure 4. (a) EPR spectra of LMoO(bdt) (**1**): experimental frozen-solution X-band spectrum (top) and simulated spectrum ($I = 0$ component only, bottom). (b) EPR spectra of LMoO(bdt) (**1**): experimental frozen-solution X-band spectrum (top) and simulated spectrum ($I = {}^5/_2$ component only, bottom). (c) EPR spectra of LMoO(bdt) (**1**): experimental frozen-solution X-band spectrum (top) and composite simulated spectrum (bottom).

EPR Spectra of Model Complexes. The EPR spectrum of LMo^VO(bdt) (**1**) exhibits a rhombic **g** tensor and an unusual **A**(^{95,97}Mo) matrix that consists of two large components ($A_1 \approx A_3$) at the extremes of the spectrum and one small component in the center, as shown in Figure 4 and Table 4. The point group symmetry of a metal complex determines which metal d orbitals are allowed to intermix. Such intermixing will determine whether or not the principal axes of the **g** and **A**(^{95,97}Mo) tensors coincide. Complexes with no symmetry elements (C_1) or with an inversion center (C_i) are not required to have any of the principal **g** and **A**(^{95,97}Mo) axes coincident, whereas

(37) Pauling, L. *The Nature of the Chemical Bond*; Cornell University Press: Ithaca, NY, 1960; p 260.

Table 4. Data for Oxo−Molybdenum(V) Complexes with Sulfur Donor Ligands (**1**−**8**)

	g_1[a]	g_2	g_3	$\langle g\rangle$	Δg[b]	A_1[c]	A_2	A_3	$\langle A\rangle$	α[d]	β	γ	ref
LMoO(bdt), **1**	2.004	1.972	1.934	1.971	0.070	50.0	11.4	49.7	37.0	0	0	0	*k*
LMoO(edt), **2**	2.018	1.970	1.939	1.975	0.079	54.6	3.3	45.5	34.5	0	0	0	*k*
LMoO{S(CH$_2$)$_3$S}, **3**	2.017	1.950	1.925	1.965	0.092	53.2	15.3	46.4	38.3	0	0	16	*k*
LMoO{S(CH$_2$)$_4$S}, **4**	2.022	1.960	1.932	1.971	0.090	52.8	15.5	43.5	37.2	18	35	0	*k*
[LMoO(S$_2$CNEt$_2$)]$^+$, **5**	1.980	1.970	1.954	1.968	0.026	64.3	30.0	13.4	35.9	0	36	0	*k*
[LMoO{S$_2$P(OEt)$_2$}]$^+$,[e] **6**	1.980	1.965	1.953	1.966	0.027	*f*	*f*	*f*	37.6	*f*	*f*	*f*	*k*
[MoO(edt)$_2$]$^-$, **7**	2.052	1.983	1.979	2.004	0.073	49.4	18.7	20.7	29.8	0	0	0	*k*
[MoO(SPh)$_4$]$^-$, **8**	2.017[g]	1.979[h]	1.979[h]	1.990	0.038	52.6[i]	23.0[j]	23.0[j]	31.5	0	0	0	36

[a] Errors ±0.001. [b] Anisotropy ($g_{max} - g_{min}$). [c] A(^{95,97}Mo), $\times 10^{-4}$ cm^{-1}). Errors $\pm 1 \times 10^{-4}$ cm^{-1} [d] α, β, and γ are Euler angles (deg). α is the angle of rotation about the z axis, β is that about the new y axis, and γ is that about the new z axis. Errors ±2°. [e] $\langle \mathbf{A}_P\rangle = 66.1 \times 10^{-4}$ cm^{-1} and $A_{P1} = A_{P2} = A_{P3} = 66.1 \times 10^{-4}$ cm^{-1}. [f] Could not be determined (see text). [g] $g_{||}$. [h] $g_{\perp}$. [i] $A_{||}$. [j] $A_{\perp}$. [k] This work.

complexes with C_2, C_s, or C_{2h} point group symmetry are required to have one of the principal **g** and **A**(^{95,97}Mo) axes coincident.[38−40] In the case of oxo−molybdenum(V) complexes of the type $LMoOX_2$, which closely approximate C_s symmetry, an Euler angle β (30−40°) for the rotation of the **g**- and **A**(^{95,97}Mo)-tensor elements has typically been observed.[38] An unusual feature of **1** is that the **g** and **A** tensors are nearly coincident in this low-symmetry (C_s) complex, where such coincidence between principal **g** and **A**(^{95,97}Mo) tensors is not required.

In general, the EPR parameters of complexes **1**−**4** are quite similar (Table 4). The g values vary little within this group, and all four exhibit a similar pattern of A(^{95,97}Mo) values, two large components on the wings of the spectrum and one small component in the center. The slight differences in the EPR parameters of these complexes can be attributed to the slight changes in their structures due to the variation in the bidentate sulfur chelate ligand. The possibility of ruffled conformations in the larger chelate rings of the bidentate sulfur ligands of **3** and **4** may lower the symmetry of these species from C_s to C_1 and thereby account for the increased rhombicity of their **g** and **A**(^{95,97}Mo) components compared to those for **1** and **2**. Lower symmetry may also lead to more than one noncoincidence angle between **g** and **A**(^{95,97}Mo) tensors, as evident from the Euler angles of **4**. However, the general similarity of the EPR parameters of **1**−**4** indicates that it is sulfur ligation of the molybdenyl group rather than the nature of the chelate skeleton that is the primary factor dictating their EPR parameters.

The cationic complexes [LMo^{V}O(S$_2$CNEt$_2$)]$^+$ (**5**) and [LMo^{V}O{S$_2$P(OEt)$_2$}]$^+$ (**6**) were electrochemically generated by one-electron oxidation of the structurally characterized [LMo^{IV}O(S$_2$CNEt$_2$)][23] and [LMo^{IV}O{S$_2$P(OEt)$_2$}][24] complexes. The dithiocarbamate and dithiophosphate ligands form four-membered delocalized chelates in cationic complexes **5** and **6**, respectively, which should possess electronic properties different from those of the dithiolate ligands of neutral complexes **1**−**4**.

Cationic [LMo^{V}O(S$_2$CNEt$_2$)]$^+$ (**5**) exhibits a rhombic EPR spectrum, and the anisotropic g and A(^{95,97}Mo) values are shown in Table 4. The principal g values and A(^{95,97}Mo) components and the pattern of A(^{95,97}Mo) values are significantly different from those of the neutral complexes **1**−**4**. The g_1 component of **5** is smaller than those in **1**−**4** and less than the free-electron value ($g_e = 2.0023$); g_2 for **5** is similar to g_2 in complexes **1**−**4**, but the g_3 component in **5** is larger than those for neutral complexes. Thus, **5** exhibits less rhombic g values than the neutral complexes **1**−**4**. The A(^{95,97}Mo) components for **5** are also different; A_1 and A_2 exhibit larger values than the corresponding A_1 and A_2 values for neutral complexes **1**−**4**, but A_3 is significantly smaller than the A_3 values of **1**−**4**. Although the *anisotropic* g and A(^{95,97}Mo) components of **5** are different from those of **1**−**4**, the *isotropic* g and A(^{95,97}Mo) values of all five compounds are similar. This similarity of the isotropic g and A(^{95,97}Mo) values among all five compounds indicates that $\langle g\rangle$ and $\langle A\rangle$ depend upon the number of sulfur donors and not their charge. The **g** and **A**(^{95,97}Mo) tensors of **5** are not coincident (Table 4).

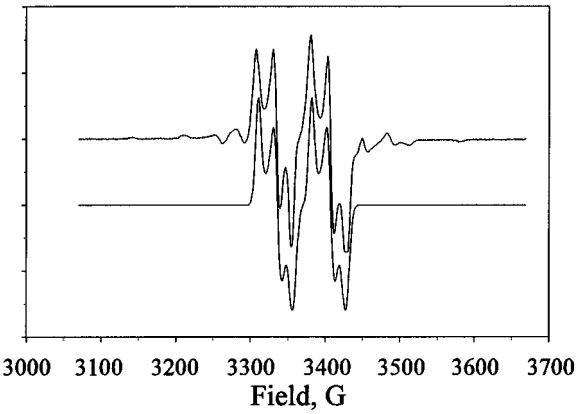

Figure 5. EPR spectra of [LMoO{S$_2$P(OEt)$_2$}]$^+$ (**6**): experimental frozen-solution X-band spectrum (top) and simulated spectrum ($I = 0$ component only, bottom).

The frozen-solution EPR spectrum of [LMo^{V}O{S$_2$P(OEt)$_2$}]$^+$ (**6**) is shown in Figure 5. The isotropic g, A(^{95,97}Mo), and anisotropic g values of **6** are identical to those of **5** (Table 4). An unusual feature of the EPR spectrum of **6** is the large ligand superhyperfine splitting (66.1×10^{-4} cm^{-1}) due to coupling with the ^{31}P ($I = {}^1/_2$) nucleus of the chelate ring. This A(^{31}P) splitting is almost twice as large as the isotropic A(^{95,97}Mo) hyperfine splitting.

The EPR spectral simulation program used in this study (QPOW) treats ligands as a perturbation; *i.e.*, ligand superhyperfine splittings are assumed to be small compared to metal hyperfine splitting. Complete EPR parameters (anisotropic A(^{95,97}Mo) hyperfine splittings) of **6** could not be simulated because isotropic A(^{31}P) ≫ A(^{95,97}Mo) splitting. However, the anisotropic g and A(^{31}P) can be simulated from the features of the EPR spectrum arising from the molecules with molybdenum atoms with $I = 0$ nuclei by assuming that the unpaired electron is localized on the ^{31}P atom. The frozen-solution EPR spectrum at 77 K (Figure 5) shows isotropic A(^{31}P) hyperfine splitting (see footnote *e* of Table 4) that is significantly larger than the isotropic A(^{31}P) splitting of 50 G previously observed for the related vanadyl dithiophosphate complex[41] and which was assigned to a σ interaction between the unpaired electron in

(38) Collison, D.; Mabbs, F. E.; Enemark, J. H.; Cleland, W. E., Jr. *Polyhedron* **1986**, *5*, 423−425.
(39) Collison, D.; Eardley, D. R.; Mabbs, F. E.; Rigby, K.; Bruck, M. A.; Enemark, J. H.; Wexler, P. A. *J. Chem. Soc., Dalton Trans.* **1994**, 1003−1011.
(40) Collison, D.; Eardley, D. R.; Mabbs, F. E.; Rigby, K.; Enemark, J. H. *Polyhedron* **1989**, *8*, 1833−1834.
(41) Miller, G. A.; McClung, R. E. D. *Inorg. Chem.* **1973**, *12*, 2552−2561.

the $d_{x^2-y^2}$ orbital and appropriate linear combinations of the two P−S σ-bonding orbitals.

Garner and co-workers have reported the synthesis, structure, and EPR spectrum of $[MoO(edt)_2]^-$ (**7**),[25] but the anisotropic $A(^{95,97}Mo)$ values of this important model compound were not reported. We have reinvestigated the nearly axial EPR spectrum of **7** and determined all the EPR parameters by simulation for the first time. The anisotropic g and $A(^{95,97}Mo)$ parameters of **7** are shown in Table 4.

Analysis of the EPR Spectra. The magnitudes of the **g**- and the **A**-tensor elements depend upon the orbital wave functions and on the relative energies of the ground and excited states.[42] The detailed form of the wave functions depends upon the point symmetry of the compound. The mixing of the metal d orbitals has been derived previously[42] for six-coordinate complexes of the type shown in Figure 2 that have two cis sulfur atoms and approximate C_s symmetry. With the molecular z axis parallel to the Mo═O bond and the y axis perpendicular to the mirror plane, the lobes of the singly occupied $d_{x^2-y^2}$ orbital lie between the atoms in the N_2S_2 plane normal to the Mo═O bond (Figure 6). The permitted d-orbital mixing within this metal-based d-orbital scheme and the relationships between the d-orbital mixing and the **g**- and **A**-tensor elements are explained elsewhere.[42,43] The **g**-tensor elements depend upon the energies and d-orbital composition of the electronic excited states. For compounds **1**−**4**, these excited state energies cannot be unambiguously determined experimentally because of the presence of overlapping low-lying sulfur to molybdenum charge transfer bands.[44] These low-lying charge transfer states and spin−orbit coupling of the sulfur atoms of the bidentate ligands[22] can account for one of the g_i values being greater than the free-electron value ($g_e = 2.0023$) for complexes **1**−**4** according to eq 2.[45−47] In eq 2, each summation is over all appropriate

$$g_i = 2.0023 - \sum\left(\frac{\zeta_{Mo}F}{\Delta E_{d-d}}\right) + \sum\left(\frac{\zeta_{Mo}G}{\Delta E_{CT}}\right) \qquad (2)$$

excited states, ζ_{Mo} is the single-electron spin−orbit coupling constant for an electron in a metal d orbital, F and G are terms that depend on the composition of the molecular orbitals in the ground and excited states and ligand spin−orbit coupling contributions, ΔE_{d-d} is the d−d transition energy, and ΔE_{CT} is the energy associated with a single-electron excitation from a filled molecular orbital of mainly ligand character to the half-filled metal d orbital of the ground state. The spin−orbit coupling term ζ_{Mo} can be estimated, and the F term can be approximated by a simple ligand field approach.[16,42] The values of the ΔE_{d-d} and ΔE_{CT} terms for complexes **1**−**4** in eq 2 cannot be unambiguously determined experimentally because it has been shown by MCD spectroscopy that the d−d bands are overlapped by the low-lying charge transfer bands.[44] Term G also contains contributions from the sulfur spin−orbit coupling constant (374 cm^{-1}). For complexes **1**−**4**, comparable contributions from the two terms of opposite sign in eq 2 could result in $g_1 \geq g_e$ (2.0023). Ligand field calculations on the W(V) center of formate dehydrogenase from *Clostridium thermoaceticum* have quantitatively demonstrated how a low-lying charge transfer state can lead to g values greater than 2.0023.[48]

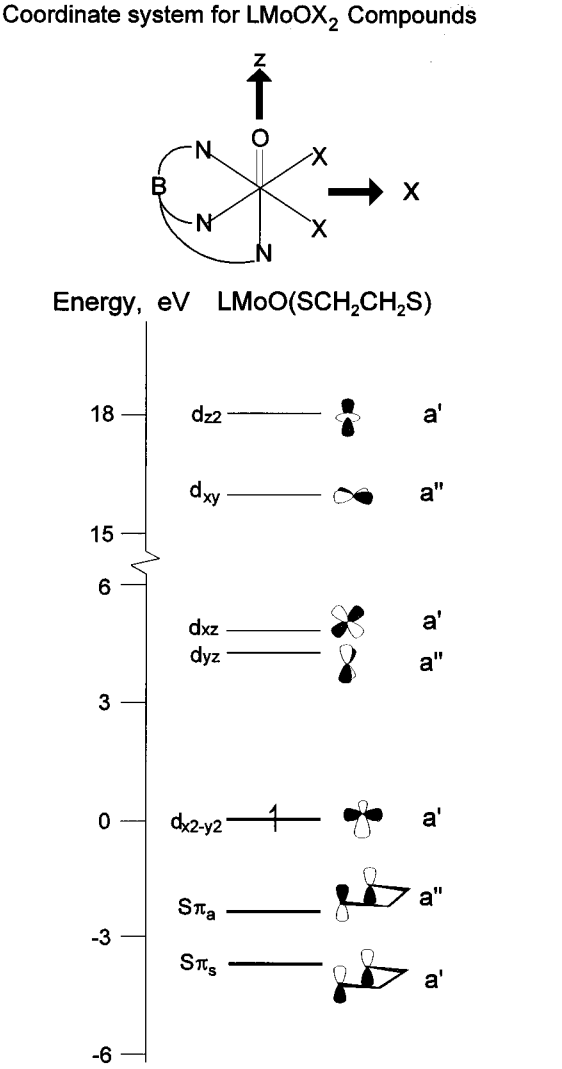

Figure 6. Partial molecular orbital diagram for $LMoO(SCH_2CH_2S)$.[44] The coordinate system is that defined previously for the analysis of EPR spectra in C_s symmetry.[43] The relationship between the coordinate systems of refs 43 and 44 are shown in Figure 13 of ref 44. Related model complexes with other chelating sulfur ligands (see text) show a similar pattern.[49,50]

The $A(^{95,97}Mo)$ hyperfine splittings of complexes **1**−**4** are similar in magnitude and exhibit a similar pattern. The principal $\mathbf{A}(^{95,97}Mo)$-tensor elements are mainly determined by the composition of the ground state.[16,42,43] The relatively small variation in the principal $A(^{95,97}Mo)$ hyperfine splitting values among **1**−**4** suggests that the ground states are not very different for these complexes. These results are supported by the Fenske−Hall calculations which predict similar ground state electronic structures for complexes **1**−**4**.[44,49]

The cationic complexes **5** and **6** exhibit $g_1 < g_e$, but g_1 is still larger than those for other oxo−molybdenum(V) complexes without sulfur donor ligands.[21,22,33] Fenske−Hall molecular orbital calculations predict similar electronic ground state functions for the neutral (**1**−**4**) and cationic (**5** and **6**) com-

(42) Mabbs, F. E.; Collison, D. *Electron Paramagnetic Resonance of d Transition Metal Compounds*; Elsevier Science Publishers B. V.: Amsterdam, 1992.
(43) Young, C. G.; Enemark, J. H.; Collison, D.; Mabbs, F. E. *Inorg. Chem.* **1987**, *26*, 2925−2927.
(44) Carducci, M. D.; Brown, C.; Solomon, E. I.; Enemark, J. H. *J. Am. Chem. Soc.* **1994**, *116*, 11856−11868.
(45) Glarum, S. H. *J. Chem. Phys.* **1966**, *41*, 1125.
(46) Garner, C. D.; Hiller, I. H.; Mabbs, F. E.; Taylor, C.; Guest, M. F. *J. Chem. Soc., Dalton Trans.* **1976**, 2258.
(47) Garner, C. D.; Mabbs, F. E. *J. Inorg. Nucl. Chem.* **1979**, *41*, 1125.
(48) Deaton, J. C.; Solomon, E. I.; Watt, G. D.; Wetherbee, P. J.; Durfor, C. N. *Biochem. Biophys. Res. Commun.* **1987**, *149*, 424−430.
(49) Carducci, M. D. Ph.D. Dissertation, University of Arizona, Tucson, AZ, 1994.

plexes.[50] However, such calculations do not give sufficiently accurate excited state energies to reliably calculate g_i values. In the absence of experimental data for these excited state energies for **5** and **6**, a more quantitative analysis of their EPR data is not possible. There are several factors that could change the anisotropic g values for cationic complexes **5** and **6**. Considerable mixing of the d orbitals in the excited states, as evident from the Euler angle β, will rotate g_1 (g_z; *vide infra*) and g_3 (g_x; *vide infra*) away from the z and x axes, respectively. This rotation about the molecular y axis (C_s symmetry) can give significantly different g_1 and g_3 for **5** and **6** because the orbital mixing may be different from the corresponding neutral complexes **1**−**4**. However, g_2 (g_y; *vide infra*) and A_2 must remain coincident with the molecular y axis in C_s symmetry. Comparison of the g values for the neutral (**1**−**4**) and cationic complexes (**5**, **6**) in Table 4 shows that g_1 and g_3 do show somewhat larger differences than does g_2. The small bite angle and electron delocalization in the four-membered chelate rings of **5** and **6** will also affect the extent of overlap of the sulfur π orbitals with the molybdenum d_π orbitals and thereby affect the anisotropic g values.

The pattern of anisotropic $A(^{95,97}\text{Mo})$ values observed for cationic complex **5** is significantly different from those of the neutral complexes **1**−**4**. The A_1 value of **5** is the largest among all of the complexes observed in this study, and the A_2 and A_3 values are larger and smaller, respectively, than the corresponding A values of the neutral complexes **1**−**4**. The observed differences in the anisotropic $A(^{95,97}\text{Mo})$ values between cationic complex **5** and the neutral complexes **1**−**4** may reflect slightly different ground state electronic structures for the neutral (**1**−**4**) and cationic (**5**, **6**) complexes. Fenske−Hall calculations predict that the electronic ground states of **5** and **6** contain about 3% d_{xz} orbital (Figure 6) character in addition to $d_{x^2-y^2}$ (75%); no significant contribution from d_{xz} is predicted for the ground states of **1**−**4**.[50]

EPR Spectral Assignments. The EPR spectrum of $[MoO(edt)_2]^-$ (**7**) exhibits nearly axial g and $A(^{95,97}\text{Mo})$ values with $g_1 > g_2 \approx g_3$ and $A_1 > A_2 \approx A_3$. The g_1 value of **7** is the largest for all the complexes investigated in this study (Table 4). The geometry of **7** is square pyramidal with the four sulfur atoms of the two chelating edt ligands occupying the basal positions;[25] the effective coordination symmetry at the molybdenum center is nearly C_{4v}. In *high-symmetry* oxo−molybdenum(V) complexes, the multiply bonded oxo ligand dominates the ligand field, and as shown by previous workers, the largest anisotropic g component and the corresponding A component are directed approximately parallel to the Mo═O bond direction.[51,52] Similar criteria have been used by Collison *et al.* to select between two alternative relationships of the **g** and **A** tensor and molecular geometry in the analysis of single-crystal EPR data on *low-symmetry* $LMoEX_2$ (E = O, S; X = Cl, NCS) complexes.[39] Adopting the same criterion for **7** and noting the similarity of the g_1 and A_1 values of this four-sulfur chelate complex (**7**) to those of the neutral two-sulfur chelate complexes (**1**−**4**) leads to the following tentative assignments for the EPR spectra of **1**−**4**: (1) g_1 is g_z and A_1 is A_z, and these elements will be aligned close to the Mo═O bond; (2) the g_2 and A_2 components can be assigned as g_y and A_y, respectively, due to the approximate C_s symmetry; (3) this leaves g_3 and A_3 as g_x and A_x, respectively. The validity of these tentative assignments awaits single-crystal EPR studies on low-symmetry oxo−molybdenum(V) complexes **1**−**4**.

General Summary of Model Compound Spectra. Comparison of the EPR parameters of complexes **1**−**6**, which have two sulfur atoms in a chelating ligand, with the parameters of complex **7**, which has four sulfur atoms from two chelating ligands, shows the typical inverse correlation between the isotropic spin-Hamiltonian parameters $\langle g \rangle$ and $\langle A \rangle$.[15,21] The isotropic g values increase and isotropic $A(^{95,97}\text{Mo})$ values decrease with increasing number of coordinated sulfur atoms. Comparison of the individual **g**-tensor components shows that all of the individual g components of the two-sulfur chelate complexes are somewhat smaller than those of the four-sulfur chelate complex **7**, with the g_3 values showing the greatest difference. The anisotropic g values of complex **7** are similar to those reported for $[MoO(mnt)_2]^-$ (mnt^{2-} = 1,2-dicyanoethylenedithiolate), where the molybdenum atom is coordinated to two dithiolene moieties through four sulfur atoms.[53] Preliminary EPR studies on other four-sulfur complexes $[MoO(bdt)_2]^-$ and $[MoO(S_2C_2(COOMe)_2)_2]^-$ show anisotropic g values are also very similar to those of complex **7**.[54,55] The general similarities of the anisotropic g values among four-sulfur complexes is further evidence that these EPR parameters are primarily determined by the number of sulfur donor atoms coordinated to the oxomolybdenum center and are nearly independent of the substituents and degree of unsaturation of the ligand skeleton.

Comparison of the anisotropic $A(^{95,97}\text{Mo})$ parameters of two-sulfur chelate complexes **1**−**5** with those of the four-sulfur chelate complex **7** shows that two-sulfur chelate complexes **1**−**5** exhibit rhombic $A(^{95,97}\text{Mo})$ hyperfine splitting, whereas the four-sulfur chelate complex **7** possesses nearly axial $A(^{95,96}\text{Mo})$ hyperfine splitting. In the absence of simulated anisotropic $A(^{95,97}\text{Mo})$ data for additional four-sulfur chelate complexes, further comparisons of the anisotropic $A(^{95,97}\text{Mo})$ hyperfine splitting patterns of two-sulfur and four-sulfur chelate complexes are unwarranted.

EPR Spectra of Sulfite Oxidase. The EPR spectra of sulfite oxidase have been extensively studied by several workers under a variety of conditions over the last 25 years,[12,27] but complete anisotropic $A(^{95,97}\text{Mo})$ hyperfine splittings were not known prior to this study. Determination of the $A(^{95,97}\text{Mo})$ hyperfine splittings is complicated by the presence of the large signal from the molybdenum centers with no nuclear spin (75% $I = 0$) and by the large ^{1}H hyperfine splitting in water. We reinvestigated the low- and high-pH forms of sulfite oxidase in D_2O in order to eliminate the splitting from exchangeable protons and made use of our previous experience with model compounds to simulate the $A(^{95,97}\text{Mo})$ hyperfine contributions to the naturally occurring mixed-isotope spectra.

The EPR spectrum of the low-pH form of sulfite oxidase (Figure 7) and the anisotropic g and $A(^{95,96}\text{Mo})$ parameters are shown in Table 5. The EPR spectrum exhibits slightly rhombic g values with $g_1 > g_e$, and the anisotropic $A(^{95,97}\text{Mo})$ values are also slightly rhombic in nature with $A_1 > A_2 \approx A_3$. Experimental determination of $\langle g \rangle$ and $\langle A \rangle$ is not possible due to the slow tumbling rate of sulfite oxidase in solution; therefore $\langle g \rangle$ and $\langle A \rangle$ were obtained by averaging the respective anisotropic g and $A(^{95,97}\text{Mo})$ components. The EPR spectrum of the low-pH form of sulfite oxidase observed in this study agrees with that originally reported,[27] and the anisotropic g values are

(50) Dhawan, I. K. Ph.D. Dissertation, University of Arizona, Tucson, AZ, 1995.
(51) Garner, C. D.; Lambert, P.; Mabbs, F. E.; King, T. J. *J. Chem. Soc., Dalton Trans.* **1977**, 1191−1198.
(52) Nilges, M. J.; Belford, R. L. *J. Magn. Reson.* **1979**, *35*, 259.
(53) Das, S. K.; Chaudhury, P. K.; Biswas, D.; Sarkar, S. *J. Am. Chem. Soc.* **1994**, *116*, 9061−9070.
(54) Oku, H.; Nakamura, A.; Johnson, M. K. Private communication.
(55) Oku, H.; Ueyama, N.; Nakamura, A. *Chem. Lett.* **1995**, 621−622.

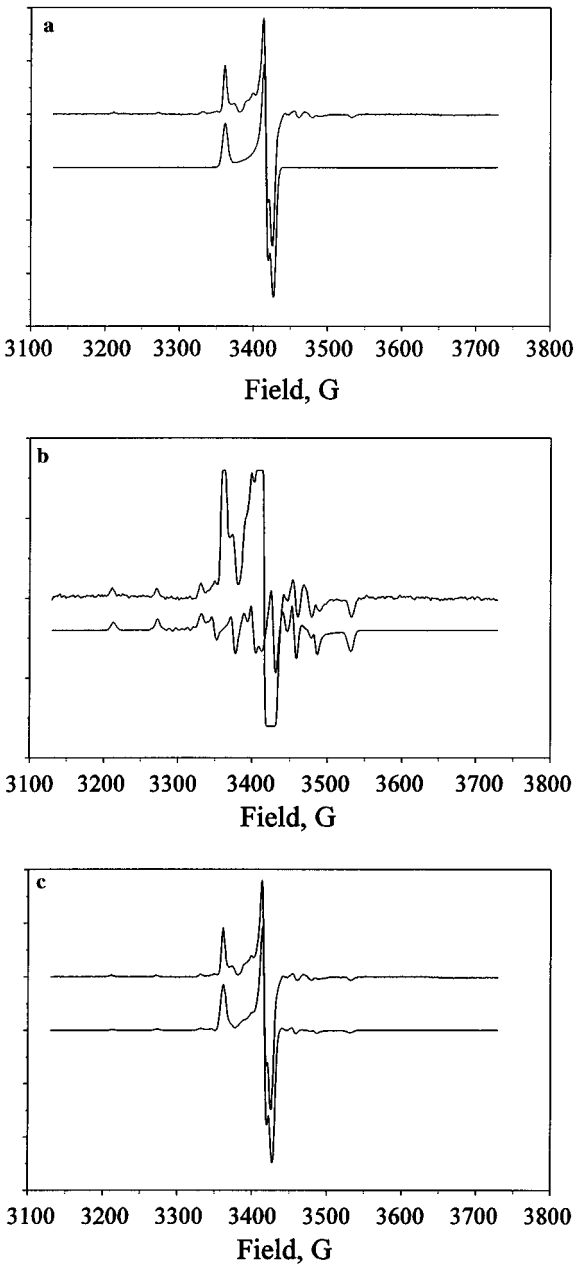

Figure 7. (a) EPR spectra of the low-pH form of the sulfite oxidase: experimental frozen-solution X-band spectrum (top) and simulated spectrum ($I = 0$ component only, bottom). (b) EPR spectra of the low-pH form of the sulfite oxidase: experimental frozen-solution X-band spectrum (top) and simulated spectrum ($I = {}^5/_2$ component only, bottom). (c) EPR spectra of the low-pH form of the sulfite oxidase: experimental frozen-solution X-band spectrum (top) and composite simulated spectrum (bottom).

consistent with those from other studies.[12] The anisotropic $A(^{95,97}\text{Mo})$ values determined here by simulation are quite different from those originally reported.[56]

The g values for the rhombic EPR spectrum of the high-pH form of sulfite oxidase (Figure 8, Table 5) also agree with those reported previously.[12,27] The g values are smaller and more rhombic than the corresponding anisotropic g values observed for the low-pH form, but both spectra show similar anisotropy. Only one component of the $\mathbf{A}(^{95,97}\text{Mo})$ tensor has been previously reported.[27] We have determined all three anisotropic $A(^{95,97}\text{Mo})$ hyperfine constants for the high-pH form of sulfite oxidase (Table 5) by simulation of the mixed-isotope spectrum. The A_1 component found in this study is in close agreement with the previous A_1 value.[27] The new values for A_2 and A_3 provide additional stringent tests for spectroscopic mimics of sulfite oxidase.

Comparison of Enzyme and Model Compound EPR Spectra. The ability to simulate the EPR spectra of systems possessing the naturally occurring mixture of molybdenum isotopes makes it possible to compare in detail **g** and $\mathbf{A}(^{95,97}\text{Mo})$ tensors for model compounds and the high- and low-pH forms of sulfite oxidase. The EPR parameters for $LMo^{V}O(bdt)$ (**1**), which possesses a *single* dithiolene ligand as proposed for the molybdenum(V) state of Mo-co, and $LMo^{V}O(edt)$ (**2**) (Table 4) reproduce g_1 and g_2 of the low-pH form of sulfite oxidase, but the g_3 values of **1** and **2** are slightly smaller than g_3 for the low-pH form of the protein. The values of $A_1(^{95,97}\text{Mo})$ for **1** and **2** are similar to that for the low-pH form of sulfite oxidase, but the large−small−large pattern of the anisotropic $A(^{95,97}\text{Mo})$ components of **1** and **2** is distinctly different from that in the low-pH form of the protein. Thus, these minimal structural models for the postulated Mo(V) state of Mo-co which possess a chelating dithiolate ligand cis to a terminal oxo group do not satisfactorily reproduce *all* of the EPR parameters of sulfite oxidase.

The complexes $[Mo^{V}O(edt)_2]^-$ (**7**) and $[Mo^{V}O(SPh)_4]^-$ (**8**) possess approximate square pyramidal geometry with four sulfur atoms cis to the terminal oxo group. Comparison of the EPR parameters of **7** and **8** (Table 4) to those of the low-pH form of the sulfite oxidase (Table 5) reveals that the $\langle g \rangle$ values and the individual anisotropic g components of **7** and **8** are all slightly larger than those of the low-pH form of sulfite oxidase. However, the pattern and magnitudes of the anisotropic $A(^{95,97}\text{Mo})$ components of **7** and **8** more closely match those of the low-pH form of sulfite oxidase than do the anisotropic $A(^{95,97}\text{Mo})$ components of **1**−**4**, which have two coordinated sulfur atoms. The $A(^{95,97}\text{Mo})$ values for **7** and **8** raise the possibility that there might be four coordinated sulfur atoms in the low-pH form of sulfite oxidase. This suggestion must be tempered, however, by the general lack of EPR data for oxo−molybdenum(V) complexes with three sulfur donor atoms. Hahn *et al.*[57] have described the synthesis of an oxo−Mo(V) complex with an S_3NO ligand system whose frozen-solution g values (1.992, 1.961, 1.953) closely resemble those of the high-pH form of sulfite oxidase. However, anisotropic $A(^{95,97}\text{Mo})$ splittings were not determined, and the proposed structure has not been verified by X-ray crystallography. The g values of the cationic two-sulfur chelate complexes (**5** and **6**) also mimic those for the high-pH form of sulfite oxidase. The close similarity of the g values of **5** and **6**, which contain nonbiological sulfur ligands, to those of the high-pH form of sulfite oxidase is a further caution against deriving active-site structures from EPR g values alone.

The recent determination of the X-ray structure of the oxidized form of aldehyde oxidoreductase (AOR) from *D. gigas* shows that the molybdenum atom is five-coordinate with two sulfur atoms being supplied by the single molybdopterin cytosine dinucleotide ligand (Figure 1b).[8] The crystal structure shows no other coordinated sulfur atoms, but the observed g values for two different Mo(V) states of this *D. gigas* enzyme (Table 5) have been interpreted on the basis of sulfo and desulfo forms of the enzyme[19] by analogy to these two proposed forms for

(56) Initial EPR studies of sulfite oxidase in D_2O at pD 7.0 showed a nearly axial spectrum with distinct $A(^{95,97}\text{Mo})$ hyperfine splittings. The EPR parameters were not simulated but taken directly from the observed spectrum (Figure 12, ref 27) as $g_{\|} = 2.000$, $g_{\perp} = 1.968$, $A_{\|} = 58.3 \times 10^{-4}$ cm^{-1}, and $A_{\perp} = 43.0 \times 10^{-4}$ cm^{-1}.

(57) Hahn, R.; Küsthardt, U.; Scherer, W. *Inorg. Chim. Acta* **1993**, *210*, 177−182.

Table 5. EPR Data for Sulfite Oxidase and *D. gigas* from AOR

	g_1[a]	g_2	g_3	$\langle g \rangle$	Δg[b]	A_1[c]	A_2	A_3	$\langle A \rangle$	α[d]	β	γ	ref
sulfite oxidase (low-pH form)	2.003	1.972	1.965	1.980	0.038	58.9							12
sulfite oxidase (low-pH form)	2.007	1.974	1.968	1.983	0.039	56.7	25.0	16.7	32.8	0	18	0	*e*
sulfite oxidase (high-pH form)	1.987	1.964	1.953	1.968	0.034	51.0							12
sulfite oxidase (high-pH form)	1.990	1.966	1.954	1.970	0.036	54.4	21.0	11.3	28.9	0	14	22	*e*
AOR *D. gigas* rapid type 2	1.988	1.970	1.964										19

[a] Errors ±0.001. [b] Anisotropy ($g_{max} - g_{min}$). [c] A(^{95,97}Mo), $\times 10^{-4}$ cm^{-1}. Errors $\pm 1 \times 10^{-4}$ cm^{-1} [d] α, β, and γ are Euler angles (deg). α is the angle of rotation about the *z* axis, β is that about the new *y* axis, and γ is that about the new *z* axis. Errors ±2°. [e] This work.

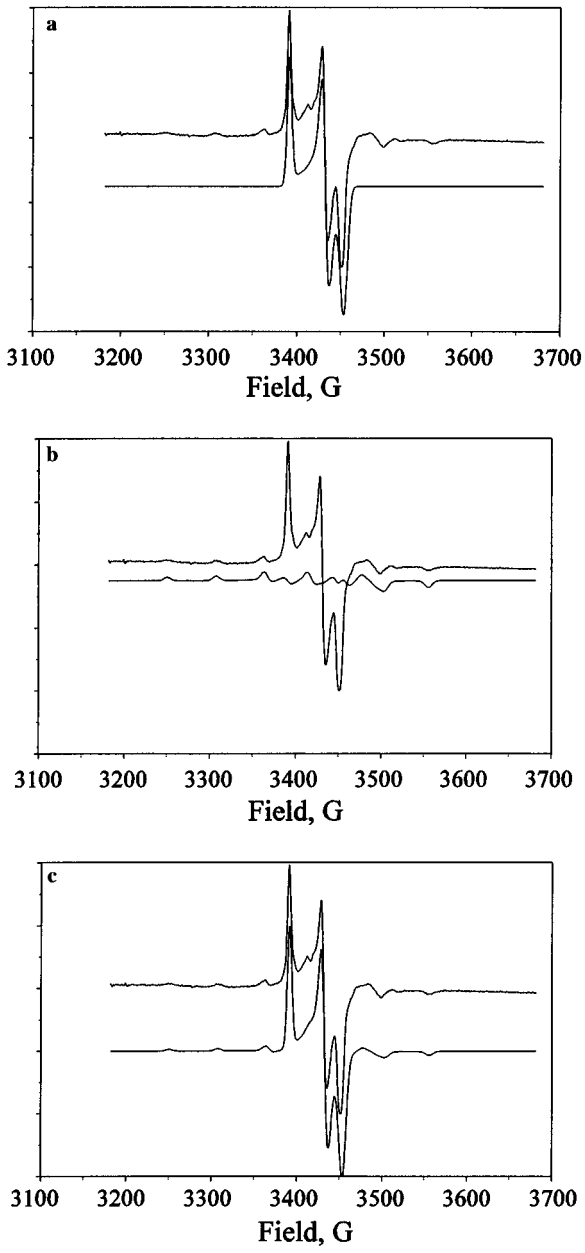

Figure 8. (a) EPR spectra of the high-pH form of the sulfite oxidase: experimental frozen-solution X-band spectrum (top) and simulated spectrum ($I = 0$ component only, bottom). (b) EPR spectra of the high-pH form of the sulfite oxidase: experimental frozen-solution X-band spectrum (top) and simulated spectrum ($I = {}^5/_2$ component only, bottom). (c) EPR spectra of the high-pH form of the sulfite oxidase: experimental frozen-solution X-band spectrum (top) and composite simulated spectrum (bottom).

the closely homologous molybdenum site of xanthine oxidase. The "slow" signal of AOR from *D. gigas* is assigned to the desulfo form of the enzyme. Its *g* values are very similar to those of the high-pH form of sulfite oxidase (Table 5). No ^{95}Mo hyperfine splittings are available for AOR from *D. gigas*, so it is not known whether the $A(^{95}\text{Mo})$ hyperfine parameters will exhibit the same splitting pattern as found here for sulfite oxidase.

Conclusions

We emphasize that $LMo^{V}O(bdt)$ is a minimal structural and spectroscopic benchmark for the binding of molybdopterin (Figure 1) to an oxomolybdenum(V) center. The benzenedithiolate ligand may be more delocalized than the *cis*-enedithiolate ($^-$SCH=CHS$^-$) ligand proposed for molybdopterin. However, this extensive systematic investigation of well-characterized model oxomolybdenum(V) compounds shows that the EPR parameters are primarily governed by the number of sulfur atoms coordinated to the oxomolybdenum(V) center rather than by unsaturation in the chelate skeleton. $LMo^{V}O(bdt)$ is not a reactivity model for molybdoenzymes because its six-coordinate stereochemistry precludes it from participating in a catalytic cycle of oxygen atom transfer and coupled electron−proton reactions as has been observed for $LMo^{VI}O_2(SPh)$ and related complexes.[58]

The successful simulation of the *natural-mixed-isotope* EPR spectra of well-characterized oxo−molybdenum complexes provides more reliable $A(^{95,97}\text{Mo})$ hyperfine parameters than directly estimating these parameters from the spectra, which is usually difficult or impossible to do. Although a wealth of EPR data has been obtained for low-symmetry oxo−molybdenum(V) complexes over the years, relatively few studies have determined the anisotropy of the $\mathbf{A}(^{95,97}\text{Mo})$ tensor and its angular relationship to the **g** tensor. Unambiguously relating the molecular framework to the EPR parameters requires a single-crystal EPR study of the paramagnetic molybdenum(V) complex diluted in a diamagnetic host lattice. Only a few such studies have been done for low-symmetry oxo−molybdenum(V) complexes.[39,42,51]

The splitting of the d orbitals in low-symmetry oxo−molybdenum(V) complexes is dominated by the oxo group.[44] The presence of sulfur donor atoms leads to low-energy charge transfer transitions from the filled sulfur π orbitals to the half-filled Mo $d_{x^2-y^2}$ orbital[44] that can give rise to EPR spectra with $g_z > g_x$, g_y and $g_z > g_e$ (eq 2).[45−47] The general similarity of the largest anisotropic *g* component and the corresponding *A* component for the neutral two-sulfur complexes (**1**−**4**) and four-sulfur complex (**7**) to the low-pH form of sulfite oxidase strongly suggests that all three possess similar electronic structures in which g_1 and A_1 are directed along the Mo=O bond. However, close inspection of the complete EPR parameters for **1**−**4** and **7** (Table 4) and those of the low-pH form of sulfite oxidase (Table 5) shows that the enzyme EPR parameters are intermediate between those of the well-characterized two-sulfur and four-sulfur systems. These differences point out the need for the synthesis and structural and spectroscopic characterization of model complexes with three thiolate ligands.

(58) Xiao, Z.; Young, C. G.; Enemark, J. H.; Wedd, A. G. *J. Am. Chem. Soc.* **1992**, *114*, 9194.

This study has provided complete EPR parameters (anisotropic g values, A(^{95,97}Mo) hyperfine splittings) of the low- and high-pH forms of sulfite oxidase from spectral simulation of the natural-mixed-isotope EPR spectra. To the best of our knowledge, these are the first complete sets of EPR parameters to be obtained for the Mo(V) state of *any* enzyme that possesses a $[Mo^{VI}O_2]^{2+}$ core in its fully oxidized form. Numerous molybdoenzymes have been studied by EPR spectroscopy,[12,14] but ^{95}Mo hyperfine splittings are usually obscured by strong splitting by exchangeable protons or are otherwise unresolvable. Complete EPR parameters have been obtained previously for xanthine oxidase, which possesses an oxidized $[Mo^{VI}OS]^{2+}$ core, by isotopic labeling of the enzyme with ^{95}Mo.[13,16] Isotopic labeling was not practically feasible for chicken liver sulfite oxidase in this work. However, recent progress in the cloning of sulfite oxidase[59] and the isolation of other bacterial molybdoenzymes (e.g. DMSO reductase)[60,61] should facilitate ^{95}Mo isotopic labeling of their molybdenum centers for direct determination of their ^{95}Mo hyperfine splittings for direct comparison to well-characterized model compounds.

(59) Garrett, R. M.; Rajagopalan, K. V. *J. Biol. Chem.* **1994**, *269*, 272−276.
(60) Bastian, N. R.; Kay, C. J.; Barber, M. J.; Rajagopalan, K. V. *J. Biol. Chem.* **1991**, *266*, 45−51.
(61) McEwan, A. G.; Ferguson, S. J.; Jackson, J. B. *Biochem. J.* **1991**, *274*, 305−307.

Acknowledgment. We thank Professor R. L. Belford for the EPR simulation package (QPOW), Dr. A. M. Raitsimring for assistance with the EPR spectra and simulations, C. Gritini for assistance with the collection of the X-ray data, Dr. A. Pacheco for preparing the samples of sulfite oxidase, and Prof. F. A. Walker, Dr. M. D. Carducci, Dr. P. Basu, and B. Westcott for helpful discussions. We are deeply grateful to Prof. R. Huber for informing us of the stereochemistry of the molybdenum center of aldehyde oxidoreductase from *D. gigas* and to Prof. D. C. Rees for information about the structure of DMSO reductase, prior to publication. Financial support from the National Institutes of Health (Grant GM-37773) and the National Science Foundation (Grant DIR-9016385 for the EPR spectrometer) is gratefully acknowledged. The X-ray structure determination was carried out in the Molecular Structure Laboratory of the University of Arizona.

Supporting Information Available: Tables of X-ray, experimental details, thermal parameters, bond distances, bond angles, and hydrogen positions for LMoO(bdt) and figures showing additional EPR spectra for sulfite oxidase and LMoO(bdt) (9 pages). Ordering information is given on any current masthead page.

IC9605276